Accurate and Reliable Thermochemistry by Data Analysis of Complex Thermochemical Networks using Active Thermochemical Tables: The Case of Glycine Thermochemistry

Journal:	*Faraday Discussions*
Manuscript ID	FD-ART-05-2024-000110.R1
Article Type:	Paper
Date Submitted by the Author:	15-Jul-2024
Complete List of Authors:	Ruscic, Branko; Argonne National Laboratory, Chemical Sciences and Engineering Division Bross, David; Argonne National Laboratory, Chemical Sciences and Engineering Division

SCHOLARONE™
Manuscripts

ARTICLE

Accurate and Reliable Thermochemistry by Data Analysis of Complex Thermochemical Networks using Active Thermochemical Tables: The Case of Glycine Thermochemistry

Received 00th January 20xx,
Accepted 00th January 20xx

DOI: 10.1039/x0xx00000x

Branko Ruscic *[a,b] and David H. Bross [a]

Active Thermochemical Tables (ATcT) were successfully used to resolve the existing inconsistencies related to the thermochemistry of glycine, based on statistically analyzing and solving a thermochemical network that includes > 3350 chemical species interconnected by nearly 35,000 thermochemically-relevant determinations from experiment and high-level theory. The current ATcT results for the 298.15 K enthalpies of formation are -394.70 ± 0.55 kJ mol^{-1} for gas phase glycine, -528.37 ± 0.20 kJ mol^{-1} for solid α-glycine, -528.05± 0.22 kJ mol^{-1} for β-glycine, -528.64 ± 0.23 kJ mol^{-1} for χ-glycine, -514.22 ± 0.20 kJ mol^{-1} for aqueous undissociated glycine, and -470.09 ± 0.20 kJ mol^{-1} for fully dissociated aqueous glycine at infinite dilution. In addition, a new set of thermophysical properties of gas phase glycine was obtained from a fully corrected nonrigid rotor anharmonic oscillator (NRRAO) partition function, which includes all conformers. Corresponding sets of thermophysical properties of α-, β-, and χ-glycine are also presented.

Introduction

Glycine, $NH_2CH_2C(O)OH$, is the simplest α-amino acid, and the only achiral proteinogenic amino acid. As an essential building block of peptides, it is clearly critical to life as we know it.[1] Aqueous glycine may also be of relevance to strategies for CO_2 sequestration.[2,3] Given its simplicity, glycine is considered to be an important pre-biotic molecule, and while its detection in interstellar space is currently at most tentative,[4-6] it has been repeatedly identified in carbonaceous chondrite meteorites.[7]

Crystalline glycine is polymorphic, with three known phases under ambient conditions: monoclinic α, trigonal χ, and a metastable monoclinic β.[8-10] In all three polymorphs and in aqueous solutions glycine assumes the tautomeric zwitterionic form, $^{+}NH_3CH_2C(O)O^{-}$, stabilized by hydrogen bonding.[11-13] As shown theoretically early on,[14-16] the zwitterion is unstable in the gas phase, where glycine assumes the canonical form.

Structure and conformers of glycine in gas phase

Out of the 24 internal degrees of freedom of glycine, three correspond to large amplitude motions: OH torsion (internal rotation about the C-O bond), NH_2 torsion (internal rotation about the C-N bond), and CH_2NH_2 (or C(O)OH) torsion (internal rotation about the C-C bond). The number of resulting conformers, their structures and their relative ordering have been the subject of both experimental[17-32] and theoretical[33-69] scrutiny for many decades. While initial ab initio calculations tended to produce results that were at variance both with each other and with experiments, as theoretical methods improved a consensus was gradually reached both on the structure of the most stable conformer (variably denoted as Gly1,[43] Ip,[44] *ttt*,[58,66] or, using the notation adopted in the present study,[70,71] *syn-anti-anti*), and on the fact that on the ground state electronic surface there are up to 8 different conformers.[55,58,65-69]

Existing thermochemistry of glycine

In spite of its potential benchmark role in both experimental and theoretical determinations of the thermochemistry of more complex amino acids, the enthalpy of formation of glycine does not appear to be sufficiently firmly established.

The critical evaluation of Pedley et al.[72] recommends the 298.15 K gas phase enthalpy of formation $\Delta_f H°_{298}$(glycine $_{(g)}$) = -392.1 ± 0.6 kJ mol^{-1}, and $\Delta_f H°_{298}$(α-glycine) = -528.5 ± 0.5 kJ mol^{-1} for the solid, same as in the predecessor evaluation by Cox and Pilcher[73] (see Table 1). The recommended enthalpy of formation of α-glycine is based on the combustion calorimetry of Huffman et al.,[74] and combined with the sublimation enthalpy determined by Svec and Clyde[75] in order to derive the value for the gas phase.

Surprisingly, the extensive TRC Tables[76,77] for organic compounds do not provide a value for glycine. The venerable NBS Tables[78] list only the solid: $\Delta_f H°_{298}$(α-glycine) = -528.1 (± 0.40)[79] kJ mol^{-1}, unchanged from the predecessor NBS Technical Note 270.[80] A subsequent critical evaluation of the available literature values for the condensed phase of glycine performed at NIST by Diaz et al.[81] selects $\Delta_f H°_{298}$(α-glycine) = -528.1 ± 0.5 kJ mol^{-1} as the 'best value', but provides no gas phase value.

The NIST Chemistry WebBook[82] typically lists all available literature values (as opposed to selecting and recommending a

---

[a] *Chemical Sciences and Engineering Division, Argonne National Laboratory, Lemont, Illinois, USA.*
[b] *e-mail: ruscic@anl.gov*

Please do not adjust margins

particular value), but for gas phase glycine it provides only a single value: $\Delta_f H^\circ_{298}$(glycine (g)) = -390.5 ± 4.6 kJ mol^{-1}, citing as the source Ngauv et al.[83] The latter authors derived the gas phase value by combining their combustion calorimetry for the solid with their calorimetric sublimation enthalpy. The single listing for the gas phase enthalpy of formation is in contrast to multiple values listed by the WebBook for the enthalpy of formation of condensed phase glycine: besides providing $\Delta_f H^\circ_{298}$(α-glycine) = -528.61 ± 0.34 kJ mol^{-1} from Ngauv et al.,[83] it also lists the more recent calorimetric determination of -527.5 ± 0.5 kJ mol^{-1} by Vasil'ev et al.,[84] as well as two older values: -528.52 ± 0.42 kJ mol^{-1} measured by Huffman et al.,[74] and -537.2 kJ mol^{-1} derived by Hutchens et al.[85] from the calorimetric determination of Tsuzuki et al.[86] A separate list of literature values for combustion enthalpies of α-glycine maintained by the WebBook, provides - in addition to the four just discussed determinations - the combustion enthalpies obtained by Emery and Benedict,[87] Wrede,[88] Fischer and Wrede,[89] and Lemoult.[90] If taken exactly as listed by the WebBook, the latter four combustion enthalpies would result in $\Delta_f H^\circ_{298}$(α-glycine) of -525.12, -523.1 ± 0.1, -523.0, and -523.61 kJ mol^{-1}, respectively.

Table 1. Experimentally based literature values for the enthalpy of formation of gas phase glycine and condensed phase α-glycine (all in kJ mol^{-1})[a]

$\Delta_f H^\circ_{298}$(glycine (g))	
-390.5 ± 4.6	Ngauv et al.[83] 1977, NIST WebBook[82] 2024
-392.1 ± 0.6	Pedley et al.[72] 1986, Cox and Pilcher[73] 1970
-393.7 ± 1.5	Dorofeeva and Ryzhova[138] 2009
$\Delta_f H^\circ_{298}$(α-glycine)	
-528.61 ± 0.34	Ngauv et al.[83] 1977, NIST WebBook[82] 2024
-528.1 ± 0.5	Diaz et al.[81] 1992
-527.5 ± 0.5	Vasil'ev et al.[84] 1991
-528.5 ± 0.5	Pedley et al.[72] 1986, Cox and Pilcher[73] 1970
-528.10 (± 0.40)	NBS Tables[78] 1982, NBS TN 270[80] 1968
-537.2 (± 1.0)	Hutchens et al.[85] 1963, Tsuzuki et al.[86] 1958
-528.52 ± 0.42	Huffman et al.[74] 1937
-525.12	Emery and Benedict[87] 1911
-523.1 ± 0.1	Wrede[88] 1911
-523.0	Fischer and Wrede[89] 1904
-523.61	Lemoult[90] 1904

[a] Values from critical evaluations are in italics

There are several even older determinations (dating from the 1890's), such as those of Berthelot[91] and Stohmann,[92,93] that are not listed by the WebBook. Indeed, these are at best only of historical significance because of their rather limited accuracies, ill-specified conditions, and poorly defined thermal units.[94]

Prima facie, the four enthalpies of formation of α-glycine found in secondary tabulations (NBS Tables,[78] Pedley et al.,[72] NIST WebBook,[82] Diaz et al.[81]) appear to cover a reasonably contained range of -(528.1 - 528.6) kJ mol^{-1}, albeit a closer scrutiny reveals that the value listed in the NIST WebBook[82] and that given by the NIST evaluation of Dias et al.[81] are technically not entirely consistent since they are just outside each other's uncertainty.[95,96] However, if one includes the values reported directly from calorimetry, the range broadens significantly to -(523 - 537) kJ mol^{-1}. Even if one excludes the four pre-1930's determinations (under the argument that they predate the full development of modern high-accuracy calorimetry[94]), the range of values for the enthalpy of formation of α-glycine still remains remarkably broad: -(527.5 - 537.2) kJ mol^{-1}.

In spite of occasional examples to the contrary,[97,98] the path of combining the enthalpy of formation of the condensed phase from combustion calorimetry with a corrected[99-101] vaporization (or sublimation) enthalpy typically produces consistent and reliable experimental results for the gas phase. However, the scatter in the experimental calorimetric values for solid glycine will clearly translate to the derived values for gas phase glycine. The reason for the scatter is unclear, given that high-quality combustion calorimetric determinations normally tend to produce mutually consistent results.

Furthermore, it appears that the determinations of the sublimation enthalpy of glycine are additionally amplifying the above problem. For example, the gas phase enthalpies of formation provided by Pedley et al.[72] and the WebBook[82] (see Table 1) differ from each other by 1.6 kJ mol^{-1}, although the selected values for α-glycine differ only by 0.1 kJ mol^{-1}, simply because Pedley et al.[72] and Ngauv et al.[83] use rather different sublimation enthalpies. Indeed, as opposed to the sublimation enthalpy of Ngauv et al.,[83] $\Delta_{sub} H^\circ_{298}$($\alpha$-glycine) = 138.1 ± 4.6 kJ mol^{-1}, Pedley et al.[72] use $\Delta_{sub} H^\circ_{298}$($\alpha$-glycine) = 136.4 ± 0.4 kJ mol^{-1} citing Svec and Clyde[75] as the source.

Part of the problem is caused by the low saturation pressure of α-glycine at room temperature, forcing the determination of its sublimation enthalpies at temperatures higher than 400 K. Indeed, Ngauv et al.[83] determined the sublimation enthalpy from calorimetric measurements in the 413 - 450 K range, averaging 131.4 kJ mol^{-1} at 432.4 K. Svec and Clyde[75] obtained 136.0 ± 0.4 kJ mol^{-1} at 455 K from Knudsen effusion measurements, and 136.4 ± 4.0 kJ mol^{-1} at 465 K from vapor pressure determinations. The other sublimation enthalpy determinations from the literature are 131 ± 2 kJ mol^{-1} obtained at 414 K by Takagi et al.[102] and 137 ± 2 kJ mol^{-1} at 419 K by de Kruif et al.[103] All of these require extrapolation to room temperature, which is not necessarily straightforward, as witnessed by the fact that beside the sublimation enthalpy extrapolated from the data of Svec and Clyde,[75] Pedley et al.[72] also considered (and ultimately rejected) a suspiciously high $\Delta_{sub} H^\circ_{298}$($\alpha$-glycine) = 153.2 ± 4.2 kJ mol^{-1}, which they extrapolated from the data of Ngauv et al.[83,104]

A reliable conversion of sublimation or vaporization enthalpies to room temperature requires reasonably accurate thermophysical properties both for the gas phase and the condensed phase, the latter depending directly on experimental determinations. The gas phase thermophysical properties can be obtained from statistical mechanics, but in case of glycine they should include all conformers and ideally be based on fully-corrected NRRAO (nonrigid rotor anharmonic oscillator) partition functions.[94,97,105]

With our partition functions (*vide infra*), the sublimation enthalpies discussed above produce 298.15 K values in the (131.4 - 137.5) kJ mol^{-1} range. When combined with the range of -(527.5 - 537.2) kJ mol^{-1} for the enthalpies of formation of

This journal is © The Royal Society of Chemistry 20xx

Please do not adjust margins

solid glycine, this produces inferred 298.15 K gas phase experimental enthalpies of formation differing by as much as 16 kJ mol^{-1}, ranging from -390.0 to -405.8 kJ mol^{-1}.

At least in principle, theoretical studies could help resolve the above difficulty. However, as opposed to abundant theoretical studies of the relative energies of the conformers of glycine, there seems to be a marked paucity of theoretical determinations of its gas phase enthalpy of formation. Clearly, one should not expect to encounter theoretical treatments of glycine using top-level state-of-the art electronic structure methods that are capable of sub-kJ mol^{-1} accuracies, such as HEAT,[107-111] W4,[112-114] FP,[115-120] FPD,[121-127] or ANL-1,[128] given that the size of this molecule tends to exceed the currently available computational capabilities. However, glycine should be fully tractable with standard mid-level composite methods, such as, for example, CBS-QB3,[129,130] CBS-APNO,[131] G3X,[132] G4,[133] and W1,[134,135] making the dearth of related literature studies somewhat surprising. While mid-level electronic structure methods are significantly less computationally demanding, they are also significantly less accurate.[95,136]

Indeed, in conjunction with initiating the relevant expansion of the Active Thermochemical Tables (ATcT) Thermochemical Network (*vide infra*), we routinely carry out our own in-house mid-level computations. Those suggest[137] the following values for $\Delta_f H°_{298}$(glycine $_{(g)}$): -396.0 (CBS-QB3), -397.3 (CBS-APNO), -395.1 (G3X), -392.1 (G4), and -399.2 kJ mol^{-1} (W1).

In the existing literature, there are at most five theoretical studies that are of relevance to the current discussion: two by Dorofeeva and Ryzhova,[138,139] and one each by Bouchoux et al.,[140] Stover et al.,[141] and Karton et al.[142]

The first study of Dorofeeva and Ryzhova[138] has produced $\Delta_f H°_{298}$(glycine $_{(g)}$) = -394.9 kJ mol^{-1} from G3X composite calculations and three isodesmic reactions at the B3LYP/6-311+G(3df,2p)//B3LYP/6-31G(d,p)[143,144] level of theory.

Incentivized by their theoretical result, these authors also proposed a revised experimental value of $\Delta_f H°_{298}$(glycine $_{(g)}$) = -393.7 ± 1.5 kJ mol^{-1}, which they obtained by combining the "best value" for $\Delta_f H°_{298}$(α-glycine) from Diaz et al.[81] with $\Delta_{sub} H°_{298}$(α-glycine) = 134.4 ± 1.5 kJ mol^{-1}. The latter sublimation enthalpy was derived by Dorofeeva and Ryzhova by converting to room temperature the 432 K value of 133.7 kJ mol^{-1}, obtained in turn as an average of determinations by Svec and Clyde,[75] Ngauv et al.,[83] Takagi et al.,[102] and de Kruif et al.[103]

Bouchoux et al.[140] reported $\Delta_f H°_{298}$(glycine $_{(g)}$) = -391.6 kJ mol^{-1} from G3(MP2)B3 computations, and Stover et al.[141] reported -384.5 kJ mol^{-1} (total atomization energy route) and -387.4 kJ mol^{-1} (isodesmic route) for the same quantity using G3(MP2) computations. In a second study, while retaining the recommended revision of the experimental value discussed above, Dorofeeva and Ryzhova[139] reported $\Delta_f H°_{298}$(glycine $_{(g)}$) = -401.4 kJ mol^{-1} using the W1U composite method.

Karton et al.,[142] on the other hand, reported the most demanding theoretical calculations of the enthalpy of formation of gas phase glycine published so far. They obtained $\Delta_f H°_{298}$(glycine $_{(g)}$) = -393.6 kJ mol^{-1} at the W2.2[134,135] level of theory, as well as -394.2 and -393.7 kJ mol^{-1} at the W1-F12 and W2-F12[145] levels of theory. They also provided $\Delta_f H°_{298}$(glycine $_{(g)}$) = -393.2 kJ mol^{-1} at what they term as a 'quasi-W4' level of theory, which assumed that higher-order corrections that would necessitate extremely demanding CCSDT(Q)/cc-pVTZ and CCSDTQ/cc-pVDZ computations, essentially cancel out over the isodesmic reaction

$NH_2CH_2C(O)OH + CH_4 \rightarrow CH_3C(O)OH + CH_3NH_2$ (R1)

The central aim of the present contribution is to obtain the best currently possible thermochemistry for glycine using the Active Thermochemical Tables approach, which employs advanced data analyses and has the ability to arbitrate between inconsistent determinations, such as those discussed earlier in this section.

Methods

Active Thermochemical Tables

Active Thermochemical Tables (ATcT) have been described in detail elsewhere.[146-149] Tersely, instead of the sequential approach to developing thermochemistry (A begets B, B begets C) that was historically used to generate virtually all traditional tabulations of enthalpies of formation, the ATcT approach is based on a distinctly different paradigm that enables the derivation of accurate and reliable thermodynamic properties for a broad range of chemical species. The ATcT approach involves constructing, statistically analysing, and solving an extensive Thermochemical Network (TN).

The construction of the TN utilizes the full breadth of available thermochemical interdependencies between the targeted chemical species, such as reaction enthalpies or free energies, adiabatic ionization energies and electron affinities, dissociative ionization onsets, etc., both from experiments and high-level theory. It should be remarked here that the TN generally does not include theoretical or experimental enthalpies of formation *per se*, since these are normally dependent on other auxiliary thermochemistry that was used in their derivation (such as enthalpies of formation of other species needed to derive the target enthalpy of formation from some computed or experimentally determined reaction enthalpy). The determinations included in the TN effectively represent a set of qualified[150] constraints that must be simultaneously satisfied by the resulting enthalpies of formation.

Before ATcT finds a simultaneous solution for all included chemical species, it conducts a statistical analysis of the TN. The aim of the latter is to identify potential outliers, i.e. determinations that within their initially assigned (a.k.a. *prior*) uncertainties are inconsistent with the prevailing epistemic content of the TN. If left intact, such determinations would unduly skew the final solution. The inconsistencies introduced by the outliers are resolved by the iterative 'worst offender'[146] procedure that generates a ranked list of 'offending' determinations and gradually increases their uncertainties, intrinsically lowering their weight in the final set of optimized enthalpies of formation. The ATcT statistical analysis of each determination is informed by the cumulative knowledge content created by the remaining determinations in the TN, and is thus effectively capable of successfully arbitrating between inconsistent determinations.

Once all the inconsistencies in the TN are resolved, ATcT solves it for simultaneously for all included species. The end result of the ATcT approach is the extraction of the best possible thermochemistry based on the existing content of the TN, characterized by significantly distributed provenances that reflect the optimal use of all currently available knowledge.

ATcT have been recently promoted to the status of U.S. DOE Office of Science Public Reusable (DOE SC PuRe) Data Resource.[151-153] The ATcT website, ATcT.anl.gov, presently attracts a million pageviews each month.[154] The most recent publicly available version of ATcT[155] results as of 2023 (ver. 1.130) provides enthalpies of formation for more than 3000 thermochemically distinct chemical species, and has been generated to accommodate the needs of a recent study of the ring-opening dynamics of the cyclopropyl radical and its cation.[156] Since then, the ATcT TN has been further expanded as a function of various interim research projects.[157-160]

The thermochemical results reported in the present study originate from ver. 1.202 of the ATcT TN, which was additionally expanded to include glycine thermochemistry, and contains more than 3350 chemical species, interlinked by nearly 35,000 determinations included in the TN. This version of the results will be shortly publicly available on the ATcT website.[161]

NRRAO thermophysical properties

Besides the TN, another important information used by ATcT are the thermophysical properties for each species. For gas phase glycine, these were obtained from NRRAO partition functions. Constructing a NRRAO partition function requires two (or more) steps. It involves the initial construction of a standard rigid rotor harmonic oscillator (RRHO) partition function using vibrational fundamentals and ground state rotational constants (rather than harmonic frequencies and equilibrium rotational constants),[94] followed by a computation of additional corrections arising from vibrational anharmonicity, rotation-vibration interaction, and centrifugal distortion, using appropriate higher order spectroscopic constants and expressions given in detail elsewhere.[94,162]

For the most stable conformer (*syn-anti-anti*) of glycine, the necessary rotational constants and fundamentals were obtained from experimental measurements,[21,23,25,26,28,32,163] while the missing higher order constants for the lowest conformer, as well as nearly all needed constants for the other conformers were obtained from computations using 2nd order vibrational perturbation theory (VPT2)[164,165] at the B3LYP/aug-cc-pVTZ level of theory. In addition, for all conformers the contributions for the three internal rotations were obtained by direct counts over the solutions of the appropriate 1D potentials. The potentials were constructed from relaxed 1D and 2D scans of the appropriate torsional dihedral angles at the B3LYP/aug-cc-pVTZ level of theory and solved using the 'universal' DVR (discrete variable representation) approach of Colbert and Miller.[166]

Electronic structure computations

The Gaussian suite of programs[167] was used for all electronic structure computations. These included mapping out the conformational space of glycine, performing related geometry optimizations, followed by relaxed 1D and 2D scans of the OH, NH_2, and CH_2NH_2 torsions for each conformer, and VPT2 computations at the B3LYP/6-31G(2df,p) and B3LYP/aug-cc-pVTZ levels of theory,[143,144,168] as well as performing routine CBS-QB3,[129,130] CBS-APNO,[131] G3X,[132] G4,[133] and W1[134,135] composite computations.

Results and discussion

In a typical situation, the addition of a new gas phase species to the ATcT TN is preceded by computing its partition function at a range of temperatures, Q°_T, and obtaining the corresponding thermophysical properties, such as isobaric heat capacities, $C^\circ_{p,T}$, entropy, S°_T, enthalpy increment, $[H^\circ_T - H^\circ_0]$, and reduced Gibbs energy, $R\ln(Q^\circ_T)$, as well as carrying out a set of exploratory mid-level composite electronic structure calculations (currently the standard set includes CBS-QB3, G3X, G4, CBS-APNO, and W1). These allow us to induct the target species to ATcT and start building the initial scaffolding that will connect the target gas phase species to the rest of the TN. The TN is subsequently augmented by relevant experimental and theoretical determinations from the literature, each of which is critically examined and – when necessary – reinterpreted.

With respect to mapping out the set of possible conformers of glycine, of note here is that their number appears somewhat dependent on the electronic structure method that is employed. For example, the popular DFT functional, B3LYP, with the 6-31G(2df,p) basis set (the model chemistry for the initial geometry optimization in G4 as well as G3X composite methods) and with the cc-pVTZ+d basis set (*idem* in the W1 composite method), results only in 7 glycine conformers that exist as true minima. Namely, in both model chemistries the highest energy conformer, *anti-perp-anti*, corresponds to an inflection on the potential energy surface, rather than an actual minimum, as can be promptly verified in corresponding relaxed 1D scans of the NH_2 torsional motion. However, at the B3LYP/aug-cc-pVTZ level of theory, all 8 different conformers can be located as minima on the potential energy surface. Consequently, for the sake of consistency across conformers, VPT2 computations at the B3LYP/aug-cc-pVTZ level of theory were uniformly employed for all conformers in order to obtain the vibrational fundamentals not available from experiments and other higher order spectroscopic constants (anharmonic constants, vibration-rotation interaction constants, centrifugal distortion constants) needed for the NRRAO partition functions.

Thermophysical properties of solid glycine

The ATcT thermophysical properties of solid glycine rely entirely on reported experimental calorimetric measurements of the heat capacities of its α-, β-, and χ-phase at extended temperature ranges, including measurements at very low temperatures.

The current ATcT partition function for α-glycine is based on the study of Rowland,[169] who critically analysed the determinations of the heat capacities of Parks et al.,[170] Hutchens et al.,[171] and Drebushchak et al.,[172] and least-squares fitted the data obtained in the latter two studies to cubic splines, following the functional form of Archer.[173] The fit of Rowland was used to generate a table of heat capacities, $C^{\circ}_{p,T}$, at 5 K increments, which were then integrated to obtain the entropies, S°_{T}, and enthalpy increments, $[H^{\circ}_{T} - H^{\circ}_{0}]$ (see Table 2).

Table 2. Thermophysical properties of crystal α-glycine at several temperatures of interest: isobaric heat capacity, $C^{\circ}_{p,T}$, entropy, S°_{T}, and enthalpy increment, $[H^{\circ}_{T} - H^{\circ}_{0}]$.[a]

T K	$C^{\circ}_{p,T}$ J K^{-1} mol^{-1}	S°_{T} J K^{-1} mol^{-1}	$[H^{\circ}_{T} - H^{\circ}_{0}]$ kJ mol^{-1}
0	0.000	0.000	0.000
50	19.266	8.939	0.318
100	43.308	30.415	1.937
150	58.945	51.053	4.508
200	72.232	69.862	7.793
250	85.633	87.399	11.735
273.15	92.114	95.265	13.793
298.15	99.125	103.634	16.183
300	99.640	104.249	16.367
350	*112.801*	*120.620*	*21.685*
400	*124.256*	*136.448*	*27.618*
450	*134.261*	*151.674*	*34.087*
500	*143.052*	*166.284*	*41.024*

[a] The values up to and including 300 K are identical to those evaluated and fitted by Rowland.[169] The values beyond 300 K (denoted in italics) are obtained by extrapolation (see text).

Thermophysical properties of α-glycine in the 410-460 K range are needed in order to be able to convert to room temperature the experimental sublimation enthalpies discussed earlier. The last cubic spline knot in the fit of Rowland[169] is at 310 K and assumes a natural spline behavior toward higher temperatures. The behavior of heat capacity, when extrapolated to higher temperatures, is close to linear, with a very gentle downward curvature. Several other possible extrapolations beyond 310 K, including a simple linear extrapolation, were also explored, and their effect on the conversion of experimental sublimation enthalpies was tested, leading to the conclusion that differences in conversion of sublimation enthalpies to 298.15 K due to different extrapolation approaches are practically negligible in view of the associated uncertainties.

The values for $C^{\circ}_{p,298}$, S°_{298}, and $[H^{\circ}_{298} - H^{\circ}_{0}]$ adopted here (see Table 2) are rather similar to those adopted in the NBS Tables (99.20 J K^{-1} mol^{-1}, 103.51 J K^{-1} mol^{-1}, and 16.180 kJ mol^{-1}, respectively).

For completeness, ATcT also includes β- and χ-glycine. The ATcT partition functions for these two polymorphs are based on differences between the heat capacities of α- and χ-glycine and of α- and β-glycine measured by Drebushchak et al.[172,174] These differences were added to the currently adopted heat capacities of α-glycine to derive the heat capacities of β- and χ-glycine (see Tables 3 and 4), and integrated to obtain the corresponding values for the entropies and enthalpy increments.

Table 3. Thermophysical properties of crystal β-glycine at several temperatures of interest: isobaric heat capacity, $C^{\circ}_{p,T}$, entropy, S°_{T}, and enthalpy increment, $[H^{\circ}_{T} - H^{\circ}_{0}]$.

T K	$C^{\circ}_{p,T}$ J K^{-1} mol^{-1}	S°_{T} J K^{-1} mol^{-1}	$[H^{\circ}_{T} - H^{\circ}_{0}]$ kJ mol^{-1}
0	0.000	0.000	0.000
50	19.382	9.062	0.321
100	43.510	30.625	1.947
150	59.223	51.361	4.530
200	72.647	70.275	7.834
250	86.801	87.989	11.816
273.15	92.068	95.907	13.887
298.15	98.591	104.266	16.275
300	99.206	104.879	16.458
350	*112.118*	*121.140*	*21.740*
400	*124.997*	*136.951*	*27.668*
450	*137.893*	*152.418*	*34.240*
500	*150.788*	*167.613*	*41.457*

Table 4. Thermophysical properties of crystal χ-glycine at several temperatures of interest: isobaric heat capacity, $C^{\circ}_{p,T}$, entropy, S°_{T}, and enthalpy increment, $[H^{\circ}_{T} - H^{\circ}_{0}]$.

T K	$C^{\circ}_{p,T}$ J K^{-1} mol^{-1}	S°_{T} J K^{-1} mol^{-1}	$[H^{\circ}_{T} - H^{\circ}_{0}]$ kJ mol^{-1}
0	0.000	0.000	0.000
50	19.826	9.412	0.333
100	43.295	31.107	1.966
150	58.390	51.637	4.523
200	71.216	70.228	7.770
250	83.857	87.461	11.643
273.15	89.880	95.151	13.654
298.15	95.894	103.287	15.978
300	96.327	103.882	16.155
350	*108.907*	*119.674*	*21.286*
400	*121.493*	*135.039*	*27.046*
450	*134.076*	*150.075*	*33.435*
500	*146.659*	*164.853*	*40.454*

Thermophysical properties of glycine (g)

The NRRAO thermophysical properties for the gas phase species denoted here as glycine (g) assume full thermal equilibration over all possible conformers. The resulting values for the isobaric heat capacity, $C^{\circ}_{p,T}$, entropy, S°_{T}, and enthalpy increment, $[H^{\circ}_{T} - H^{\circ}_{0}]$ are given at several temperatures of interest in Table 5.

Table 5. NRRAO thermophysical properties of gas phase glycine (g), fully thermally equilibrated over all conformers at several temperatures of interest: isobaric heat capacity, $C°_{p,T}$, entropy, $S°_T$, and enthalpy increment, $[H°_T - H°_0]$.

T K	$C°_{p,T}$ $J K^{-1} mol^{-1}$	$S°_T$ $J K^{-1} mol^{-1}$	$[H°_T - H°_0]$ $kJ mol^{-1}$
0	0.000	0.000	0.000
50	40.547	213.951	1.808
100	51.75	245.263	4.099
150	64.952	268.734	7.015
200	77.466	289.163	10.581
250	88.736	307.681	14.741
273.15	93.606	315.754	16.852
298.15	98.677	324.171	19.256
300	99.046	324.783	19.438
350	108.774	340.786	24.636
400	118.371	355.936	30.314
450	128.548	370.455	36.482
500	140.506	384.595	43.198

Conformers of gas phase glycine

In addition to fully equilibrated gas phase glycine, glycine (g), *vide supra*, ATcT also treats each possible conformer of glycine as a separate chemical species using the split-species approach.[94,105,175] The split-species approach ensures that the thermophysical properties of fully equilibrated glycine (g) correspond at each temperature to a correctly weighted sum over the individual conformers, with weights reflecting their relative equilibrium concentrations.

As mentioned earlier, the corresponding NRRAO partition functions utilize the spectroscopic constants appropriate for each conformer, with the exception of the three internal rotors, the contributions of which are computed by direct count of torsional levels that were obtained by solving the appropriate hindered rotor potential.

However, each of these torsional potentials (and the resulting torsional levels) belongs to at least two conformers, and thus a straightforward full state count for each individual conformer would overestimate the contributions of torsional modes. The standard solution used in ATcT for cases where there is more than one conformer (or isomer) on the same potential energy surface is to compute the appropriate fractional weights for each torsional mode. Thus, in computing the contributions to the partition function of individual conformers of glycine, the fractional weight[176] of each torsional level was obtained by integrating the square of each vibrational wavefunction (also obtained via DVR[166]) over the relevant potential well, where apexes of the appropriate transition states between conformers were used to define the integration limits along the corresponding torsional mode.

Figure 1 depicts the shapes of the 8 conformers and their energies (in cm^{-1}, relative to the most stable conformer). The listed energies are obtained by ATcT by considering all relative energy entries in the TN, which consist of results obtained from the mid-level computations (*vide supra*), together with relevant experimental and theoretical values from the literature.[13,21,24-27,29,30,44,46,48,51,55,58,59,61,63,67-69] Given that even unexpensive density functional computations produce very reasonable differences in conformational electronic energies,[65] uncertainties in (anharmonic) zero-point energies (and, in particular, in contributions of torsional modes) are bound to significantly contribute to the overall uncertainties.[177]

On the ground electronic state of gas phase glycine there are altogether 12 minima corresponding to 8 conformers. Each of the four C_s conformers (*syn-anti-anti*, *syn-anti-syn*, *anti-anti-anti*, and *anti-anti-syn*) corresponds to a distinct minimum, while each of the C_1 conformers (*anti-syn-syn*, *syn-perp-anti*, *syn-perp-syn*, and *anti-perp-anti*) possesses two enantiomeric minima. In the latter group, the primary distortion toward C_1 symmetry originates from the *gauche* torsional position of the NH_2 group, with the rest of the molecule relaxing slightly because of the loss of the plane of reflection, but otherwise staying relatively close to a symmetric arrangement.

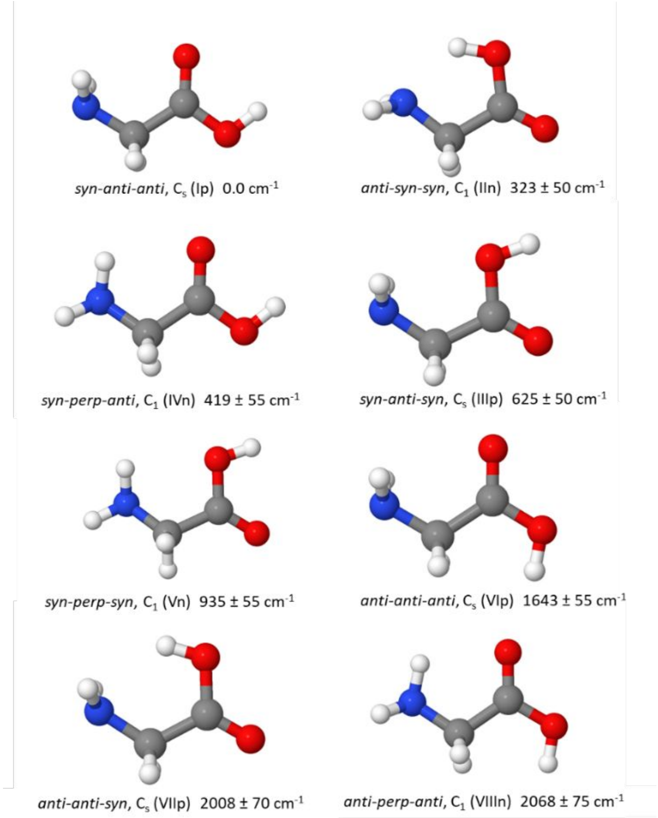
syn-anti-anti, C_s (Ip) 0.0 cm^{-1}

anti-syn-syn, C_1 (IIn) 323 ± 50 cm^{-1}

syn-perp-anti, C_1 (IVn) 419 ± 55 cm^{-1}

syn-anti-syn, C_s (IIIp) 625 ± 50 cm^{-1}

syn-perp-syn, C_1 (Vn) 935 ± 55 cm^{-1}

anti-anti-anti, C_s (VIp) 1643 ± 55 cm^{-1}

anti-anti-syn, C_s (VIIp) 2008 ± 70 cm^{-1}

anti-perp-anti, C_1 (VIIIn) 2068 ± 75 cm^{-1}

Figure 1. The conformers of gas phase glycine, depicted in their inertial (Wigner) frames: axis *a* is the abscissa, *b* is the ordinate, and *c* is perpendicular to the plane of the figure. The current nomenclature for the conformers is explained in ref. 70, while, for reference purposes, the nomenclature used in ref. 44 is given in parentheses. The relative energies and their uncertainties are from ATcT.

Here we would like to briefly discuss some of the peculiarities of topological relations of select conformers of glycine, particularly those of C_1 symmetry. For ease of illustrating the points raised in the discussion, unless explicitly noted differently, we will refer to energy differences obtained from

B3LYP/aug-cc-pVTZ relaxed torsional scans, the accuracy of which is admittedly limited and should be understood primarily as a qualitative indicator.

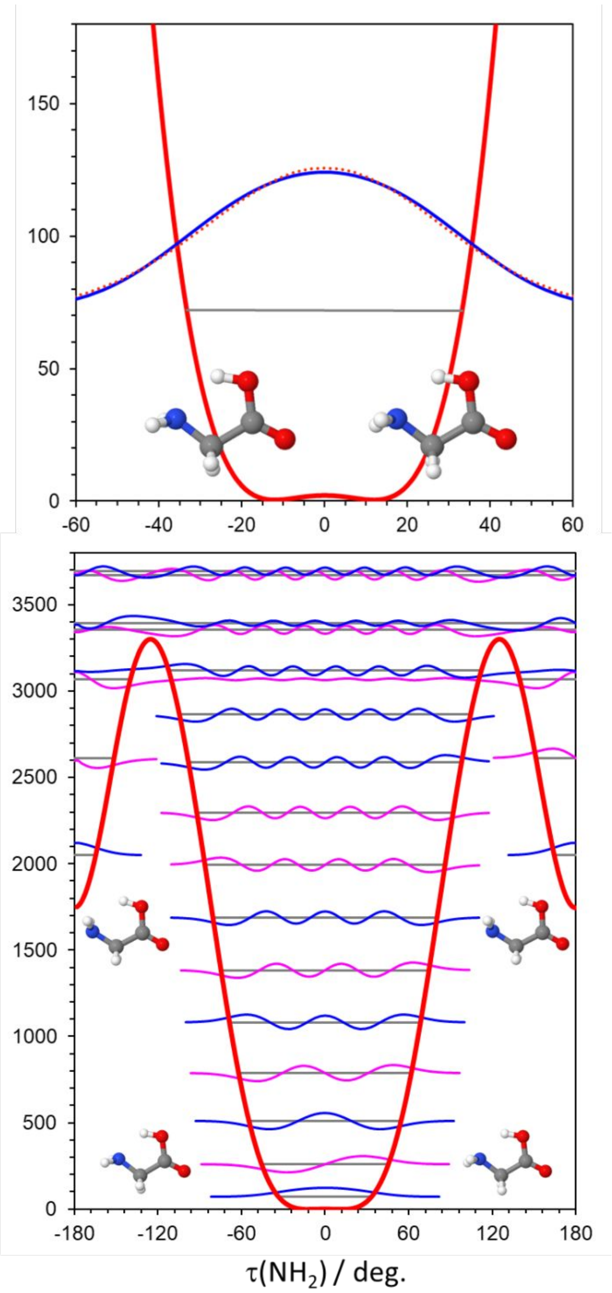

Figure 2. The 1D potential energy of the NH_2 torsion of the *anti-syn-syn* conformer. Lower panel: overall view, including the torsional wavefunctions and the higher *anti-anti-syn* conformer. Upper panel: a detailed view of the bottom of the potential well with the two enantiomeric equilibrium structures of the *anti-syn-syn* conformer separated by a small barrier that is well below the ground state level; the ground state torsional function (blue trace) is almost identical to a Gaussian wave packet of C_s symmetry (red dotted line).

The equilibrium geometry of the second conformer, *anti-syn-syn*, both at the B3LYP/aug-cc-pVTZ and B3LYP/6-31G(2df,p) level of theory, displays a very slightly *gauche* NH_2 group. However, the barrier separating the two resulting enantiomeric minima is not only quite low (of the order of just a few cm^{-1}), but also significantly lower than the energy of the ground state level of this conformer (by about 70 cm^{-1} on the B3LYP/aug-cc-pVTZ 1D potential for the NH_2 torsion, see Figure 2). Consequently, the two enantiomeric structures of *anti-syn-syn* are experimentally undistinguishable, and the effective geometry of this conformer is C_s even in the ground state, in full accord with the conclusions from the advanced Focal Point study of Kasalova et al.[178]

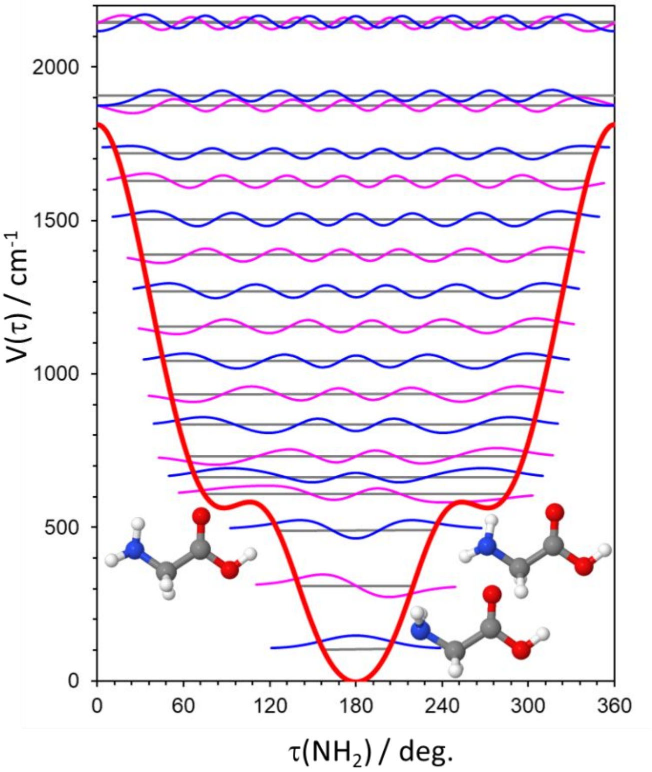

Figure 3. The 1D potential energy of the NH_2 torsion of the *syn-anti-anti* conformer, which leads to two higher (enantiomeric) shallow minima of the *syn-perp-anti* conformer. The lowest torsional level associated with the *syn-perp-anti* conformer is appreciably above the small barrier separating this conformer from the deep *syn-anti-anti* well, and the corresponding torsional wavefunction is delocalized over all three minima.

In the third conformer, *syn-perp-anti*, the two enantiomeric minima are mutually separated by a rather high barrier (~1250 cm^{-1}), but each of these minima is separated from the much deeper well of the most stable conformer, *syn-anti-anti*, by a rather low barrier (< 20 cm^{-1}, see Figure 3). Furthermore, the lowest torsional level that can be rightfully associated with the *syn-perp-anti* conformer (and thus designated as its ground state level) is above the latter barrier (by ~25 cm^{-1}). Consequently, even in its ground state, this conformer exists in the *syn-perp-anti* conformation no more than 35% of the time, spending 65% of the time above the deeper *syn-anti-anti* well, as suggested by the integrated amplitudes of the corresponding wavefunction. The proportion of time spent in the *syn-perp-anti* conformation changes with each subsequent torsional level, and, for example, increases to 69%, 59%, 45%, and 55%, for the next four torsional levels, eventually hovering at ~60% at sufficiently high energies.

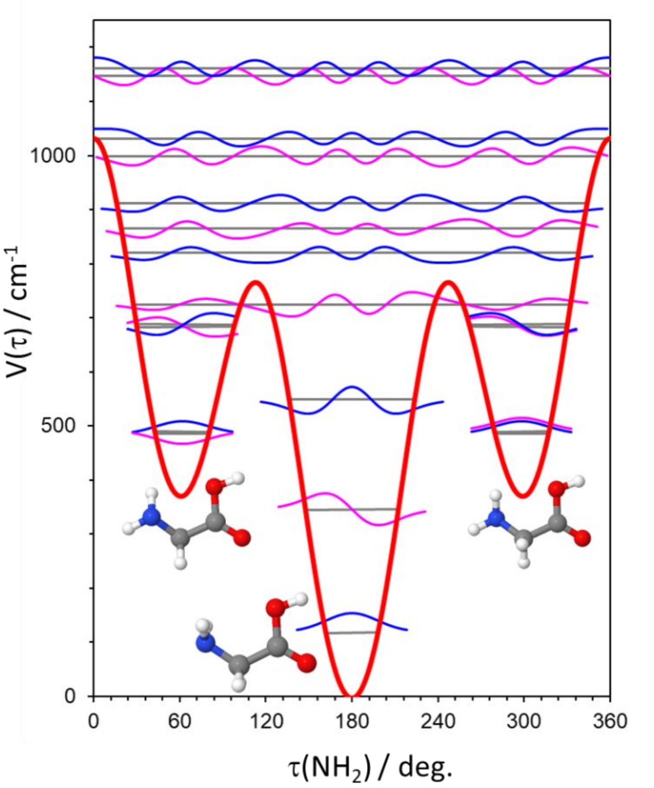

Figure 4. The 1D potential energy of the NH_2 torsion depicting the two enantiomeric *syn-perp-syn* minima and the deeper *syn-anti-syn* minimum.

In the fifth conformer, *syn-perp-syn*, the NH_2 torsion connects the ground states of each of its two enantiomers with the more stable *syn-anti-syn* conformer through barriers (~280 cm^{-1}) that are lower than the barrier (~550 cm^{-1}) separating the two enantiomers of *syn-perp-syn* (see Figure 4). The lowest pair of torsional levels associated with the *syn-perp-syn* conformer is essentially entirely located in that well and is inversion-split (< 0.1 cm^{-1}), while the next torsional level is essentially located in the well of the more stable *syn-anti-syn* conformer. The next two torsional levels belong primarily to the *syn-perp-syn* conformer, but already appear to tunnel slightly into the *syn-anti-syn* well (18% and 3%, respectively), and the following torsional level even more pronouncedly so (only 24% of the time located in the *syn-perp-syn* enantiomeric wells). While the next torsional level is already above the barrier separating the two conformers, it is still more than half of the time (56%) located in the enantiomeric *syn-perp-syn* wells, as are subsequent torsional levels (82%, 62%, 62%, 79%, 65%, etc.).

The NH_2 torsion of the highest conformer, *anti-perp-anti*, connects each of its two enantiomers with the *anti-anti-anti* conformer via an extremely small barrier (< 5cm^{-1}), while the two enantiomeric wells are separated by a more substantial barrier (~1280 cm^{-1}, see Figure 5). The lowest torsional level that can be associated with the *anti-perp-anti* conformer is, in fact, above the barrier separating *anti-perp-anti* from *anti-anti-anti* (by ~35 cm^{-1}), leading to a situation not dissimilar to that described earlier for the ground state of the *syn-perp-anti* conformer: even in its ground state the *anti-perp-anti* conformer spends only 32% of the time above its enantiomeric wells. Surprisingly, in subsequent torsional levels this increases (59%, 54%, 45%, 48%, 56%, etc.), eventually achieving a more consistent ~60% level at higher energy.

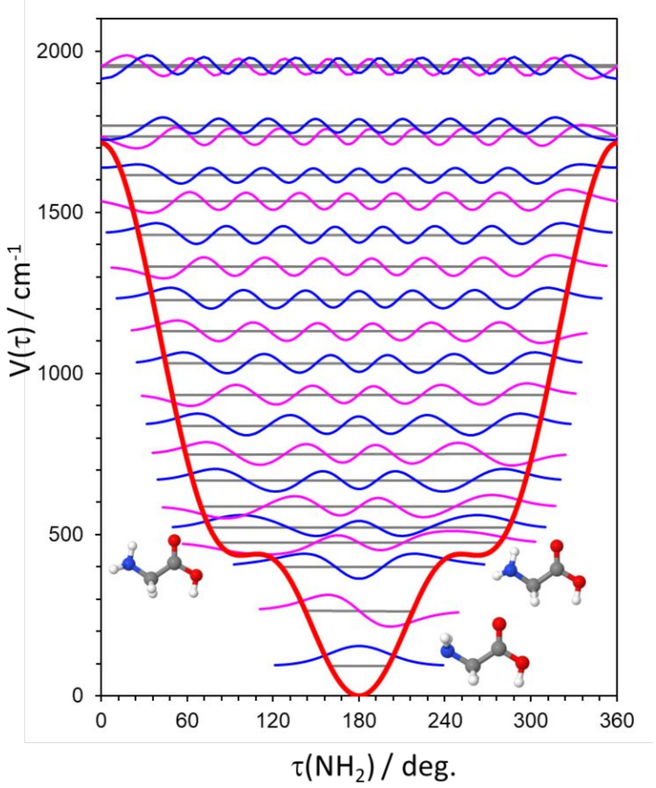

Figure 5. The 1D potential energy of the NH_2 torsion depicting the two very shallow minima of the enantiomeric *anti-perp-anti* minima and the deeper *anti-anti-anti* minimum.

ATcT thermochemistry of glycine

Table 6 provides the current ATcT enthalpies of formation of glycine in various phases of interest at 298.15 K and – when applicable – at 0 K.

Table 6. Current ATcT enthalpies of formation of glycine in various phases, based on TN ver. 1.202 (all in kJ mol^{-1})

Species	**0 K**	**298.15 K**	**uncert.**
glycine (g)	-377.67	-394.70	± 0.55
glycine (cr, α)	-508.27	-528.37	± 0.20
glycine (cr, β)	-508.04	-528.05	± 0.22
glycine (cr, χ)	-508.34	-528.64	± 0.23
glycine (aq, undiss.)	÷	-514.22	± 0.20
glycine (aq)	÷	-470.09	± 0.20

For the condensed phase of glycine, the ATcT TN contains all post-1930 experimentally determined combustion enthalpies discussed in the Introduction. The resulting ATcT enthalpy of

Please do not adjust margins

formation of the primary (α) polymorph of condensed phase glycine is $\Delta_fH°_{298}$(α-glycine) = -528.37 ± 0.20 kJ mol^{-1}.

Comparing to values listed in Table 1, it is evident that the enthalpy of formation determined by Huffman et al.[74] (-528.52 ± 0.42 kJ mol^{-1}), which is the basis for the value recommended by Cox and Pilcher[73] and Pedley et al.[72] (-528.5 ± 0.5 kJ mol^{-1}), and the value determined by Ngauv et al.[83] (-528.61 ± 0.34 kJ mol^{-1}) are both rather close to the current (and more accurate) ATcT value. Within their uncertainties, the recommendations given by Diaz et al.[81] (-528.1 ± 0.5 kJ mol^{-1}), and by the NBS Tables[78] (-528.10 ± 0.40 kJ mol^{-1}) are also entirely compatible. With the uncertainty originally assigned by the authors, the more recent value of Vasil'ev et al.[84] (-527.5 ± 0.5 kJ mol^{-1}) is only marginally compatible, since there is technically a modest gap in the overlap within combined uncertainties. However, with a revised uncertainty of ± 1 kJ mol^{-1} (assigned as a more realistic *prior* to the corresponding combustion calorimetry entry in the TN, *vide infra*), the determination of Vasil'ev et al. becomes entirely congruent with the current ATcT result.

Not entirely unexpectedly, the current ATcT enthalpy of formation for α-glycine rules out the higher (less negative) pre-1930's values of Emery and Benedict[87] (-525.12 kJ mol^{-1}), Wrede[88] (-523.1 kJ mol^{-1}), Fischer and Wrede[89] (-523.0), and Lemoult[90] (-523.61 kJ mol^{-1}).

When compared to the current ATcT value, the largest outlier in Table 1 seems to be the significantly more negative value inferred by Hutchens et al.[85] (-537.2 kJ/mol) from the calorimetry of Tsuzuki et al.[86] In rechecking the genesis of that value, one finds that Tsuzuki et al. indeed reported a heat of combustion value for glycine of -966.1 ± 0.9 kJ mol^{-1} (-230.9 ± 0.2 kcal mol^{-1}) at constant volume (necessitating an additional small correction of 0.6 kJ mol^{-1} to constant pressure)[179], which appears to be significantly less exothermic than any other experimental combustion enthalpy of α-glycine included in the TN, and is consequently in substantial disagreement with the current ATcT result $\Delta_{combust}H°_{298}$(α-glycine) = -973.08 ± 0.19 kJ mol^{-1}.

With very few exceptions, the provenances of ATcT enthalpies of formation are distributed over a number of determinations extant in the TN, and can be extracted by performing a variance decomposition analysis.[180] It is useful to point out here that a distributed provenance imparts an enhanced degree of reliability to the corresponding ATcT result, since it signifies that the ATcT value does not uniquely depend on any particular determination. The latter aspect of the ATcT provenances is in significant contrast to provenances of sequentially-developed thermochemical values, which typically critically depend on a single determination that was selected as being 'the best' by the evaluator and used for the derivation of the enthalpy of formation of the target species.

As one might have already guessed by simply comparing the current ATcT enthalpy of formation of α-glycine with the historical values given in Table 1, the internal statistical analysis of ATcT favors the combustion calorimetry of Ngauv et al.[83] and Huffman et al.[74] once all of the glycine-related thermochemical determinations that are included in the TN (including theoretical, *vide infra*) are considered in earnest. Indeed, the provenance analysis indicates that the primary contributors to the ATcT value of the enthalpy of formation of α-glycine are the calorimetric determination of Ngauv et al.[83] (67%) and of Huffman et al.[74] (18%), with a small contribution (3%) from the determination by Vasil'ev et al.[84] (noting again that the uncertainty of the latter combustion enthalpy was reevaluated prior to entry in the ATcT TN to ± 1.0 kJ mol^{-1}, double the authors' original estimate of ± 0.5 kJ mol^{-1}).

For the sake of completeness, the ATcT includes χ- and β-glycine. Their enthalpies of formation, also given in Table 6, essentially rely internally on the current ATcT value for α-glycine, combined with the relevant entries in the ATcT TN defining the enthalpic differences between the three polymorphs, as reported by Perlovich et al.[9] and Drebushchak et al.[172] from differences in dissolution enthalpies.

In a similar vein, Table 6 also lists the 298.15 K enthalpies of formation of two thermodynamically-definable forms of aqueous glycine. The glycine $_{(aq,\ undiss.)}$ species refers to a hypothetical glycine that is dissolved in water, but not yet dissociated, while glycine $_{(aq)}$ refers to fully dissociated aqueous glycine at infinite dilution. Parenthetically, the enthalpy of formation of glycine $_{(aq)}$ is identical to the enthalpy of formation of the glycinate NH2CH2C(O)O$^-$ $_{(aq)}$ anion, since by thermochemical convention the aqueous counterion H$^+$ $_{(aq)}$ has zero enthalpy of formation.[94,181]

The thermochemical relationship between α-glycine and aqueous undissociated glycine $_{(aq,\ undiss.)}$ is in the TN defined via free energies and enthalpies of solution,[182] from a large number of experimental determinations.[169,183-192] Of these, the critical evaluation of Rowland,[169] and the experimental determinations of Miller and Smith-Magowan[187] and of Spink and Wadso,[184] appear most accurate and are consequently the primary contributors to the resulting ATcT value for $\Delta_fH°_{298}$(glycine $_{(aq,\ undiss.)}$).

Mutatis mutandis, the thermochemistry of fully dissociated aqueous glycine $_{(aq)}$ at infinite dilution is defined in the ATcT TN relative to undissociated aqueous glycine $_{(aq,\ undiss.)}$ via the experimental determinations[193-198] that relate to the second dissociation constant of aqueous glycine.[199] According to the variance decomposition, the ATcT enthalpy of formation of glycine $_{(aq)}$ is most strongly influenced by the quite accurate determinations by Hamborg et al.,[197] Datta and Grzybowski,[195] and Owen.[193]

With respect to the thermochemistry of aqueous glycine, of note is that the difference between the 298.15 K enthalpy of formation of α-glycine and glycine $_{(aq,\ undiss.)}$ implied by the corresponding values in the NBS Tables, 14.11 (± 0.40) kJ mol^{-1}, is nearly identical to the current ATcT value, 14.15 ± 0.01 kJ mol^{-1}. Similarly, the difference between the 298.15 K enthalpy of formation of α-glycine and glycine $_{(aq)}$ from the NBS Tables, 58.32 (± 0.40) kJ mol^{-1}, is essentially the same as the ATcT value, 58.29 ± 0.04 kJ mol^{-1}.

The ATcT enthalpy of formation of gas phase glycine is $\Delta_fH°_{298}$(glycine $_{(g)}$) = -394.70 ± 0.55 kJ mol^{-1}. The ATcT value is 2.6 kJ mol^{-1} more stable than the value of Pedley et al.[72] (-392.1 ± 0.6 kJ mol^{-1}) and ~4.2 kJ mol^{-1} more stable than the value of Ngauv et al.[83] (-390.5 ± 4.6 kJ mol^{-1}), although the significantly

Please do not adjust margins

larger uncertainty of the latter value allows for some overlap. In contrast to these two literature values, the recent experimentally-based revised value of Dorofeeva and Ryzhova[138] of -393.7 ± 1.5 kJ mol^{-1} has, within its own uncertainty, a comfortable overlap with the current ATcT value. It should be emphasized here that with respect to the thermochemistry of gas phase glycine, the ATcT TN includes both experimental and theoretical determinations. The experimental path to gas phase glycine in the ATcT TN relies on α-glycine and involves determinations of sublimation enthalpies discussed in the Introduction. In terms of theoretical determinations, in addition to reaction (R1) given earlier, the ATcT TN includes the following isodesmic reaction:

$NH_2CH_2C(O)OH + CH_3CH_3 \rightarrow CH_3C(O)OH + CH_3CH_2NH_2$ (R2)

For both reactions the ATcT TN includes the computational 0 K energies obtained at five mid-level composite calculations carried in-house as discussed in the Methods section. Perhaps more importantly, for reaction (R1) the TN contains the 0 K reaction energy that is based on the quasi-W4 value for glycine of Karton et al.[142] and W4 values for the other reactants from the W4-11 dataset.[200] The ATcT TN also includes the 0 K total atomization energies at the W1-F12, W2-F12, and W2.2 level of theory obtained by Karton et al.[142]

The variance decomposition reveals that the primary provenance of the ATcT enthalpy of formation of gas phase glycine is from experimental data. Consequently, the ATcT value for the enthalpy of formation of gas phase glycine relies primarily on the ATcT enthalpy of formation of α-glycine, combined with the ATcT sublimation enthalpy $\Delta_{sub}H°_{298}(\alpha\text{-glycine}) = 133.68 \pm 0.55$ kJ mol^{-1}. Variance decomposition indicates that the two primary contributors to the latter are the determinations by Ngauv et al.[83] (38%) and by Takagi et al.[102] (9%).

Theory has a secondary, but definitely non-negligible contribution to the ATcT enthalpy of formation of gas phase glycine. The most relevant theoretical determination is the isodesmic reaction (R1), where, according to variance decomposition analysis, the primary contributor is the quasi-W4 reaction energy of Karton et al.[142] (14%). In particular, the current ATcT 0 K enthalpy of reaction (R1) is $\Delta_rH°_0(R1) = 19.33 \pm 0.56$ kJ mol^{-1}, while the theoretical value obtained by combining the quasi-W4 enthalpy of formation of glycine[142] with W4 enthalpies of formation from the W4-11 database[200] is 19.1 kJ mol^{-1} (cf. to the rather similar 19.4 kJ mol^{-1} at the W2.2 level of theory). Evidently, the current ATcT value and the quasi-W4 value (as well as the W2.2 value) are in excellent agreement, differing only by 0.2 kJ mol^{-1}.

In retrospect, it appears that the theoretical result of Karton et al.[142] for reaction (R1) (which slightly gains additional statistical significance by the rather similar mid-level computational values for reaction (R1), which range between 18.9 and 20.4 kJ mol^{-1}), helps guide the iterative process of convergence to the final ATcT results listed in Table 4. Namely, during the ATcT statistical analysis of the TN content, the existence of theoretical results for reaction (R1) in the TN influences the internal consistency checks and helps pruning down the set of possible enthalpy/sublimation enthalpy combinations to a feasible subset that is consistent with the enthalpy of formation of gas phase glycine implied by reaction (R1), thus helping the process of arbitration between inconsistent determinations surrounding α-glycine.

Conclusions

Given the fact that the entries in the ATcT TN consist primarily of curated[201] thermochemically-related determinations from the literature, enhanced by additional in-house computations, the ATcT approach is arguably a data-mining approach that is capable of arbitrating between inconsistent determinations. In the case of glycine, ATcT successfully resolved the existing inconsistencies in literature data, producing final enthalpies of formation of gas phase glycine, all three polymorphs of solid glycine, and two thermodynamically distinguishable aqueous forms, as given in Table 6. These results correspond to the most accurate thermochemical values for glycine currently in existence.

Conflicts of interest

There are no conflicts to declare.

Acknowledgements

This work was supported by the U.S. Department of Energy, Office of Science, Office of Basic Energy Sciences, Division of Chemical Sciences, Geosciences and Biosciences under Contract No. DE-AC02-06CH11357, through the Gas Phase Chemical Physics Program (BR) and the Computational Chemical Sciences Program (DHB). The Active Thermochemical Tables are a U.S. Department of Energy Office of Science Public Reusable Research (DOE SC PuRe) Data Resource.[151]

Notes and references

1 A. L. Lehninger, D. L. Nelson, M. M. Cox and A. A. Hoskins, "Principles of Biochemistry", 8th Ed., Macmillan: Austin 2021

2 X. Ma, V. S. Bryantsev and S. Roy, *Cell Rep. Phys. Sci.*, 2023, **11**, 101642/1-20.

3 H. Lyu, O. I.-F. Chen, N. Hanikel, M. I. Hossain, R. W. Flaig, X. Pei, A. Amin, M. D. Doherty, R. K. Impastato, T. G. Glover, D. R. Moore and O. M. Yaghi, *J. Am. Chem. Soc.*, 2022, **144**, 2387–2396

4 Y.-J. Kuan, S. B. Charnley, H.-C. Huang, W.-L. Tseng and Z. Kisiel, *Astrophys. J.*, 2003, **593**, 848-867.

5 L. E. Snyder, F. J. Lovas, J. M. Hollis, D. N. Friedel, P. R. Jewell, A. Remijan, V. V. Ilyushin, E. A. Alekseev and S. F. Dyubko, *Astrophys. J.*, 2005, **619**, 914-930.

6 M. Lattelais, F. Pauzat, J. Pilmé, Y. Ellinger and C. Ceccarelli, *Astron. Astrophys.*, 2011, **532**, A39/1-7.

7 M. A. Sephton, *Nat. Prod. Rep.*, 2002, **19**, 292-311.

8 Y. Iitaka, *Nature*, 1959, **183**, 390-391.

9 G. L. Perlovich, L. K. Hansen and A. Bauer-Brandl, *J. Therm. Anal. Cal.*, 2001, **66**, 699-715.

10 E. V. Boldyreva, V. A. Drebushchak, T. N. Drebushchak, I. E. Paukov, Y. A. Kovalevskaya and E. S. Shutova, *J. Therm. Anal. Cal.*, 2003, **73**, 409-418; E. V. Boldyreva, V. A. Drebushchak, T. N. Drebushchak, I. E. Paukov, Y. A. Kovalevskaya and E. S. Shutova, *J. Therm. Anal. Cal.*, 2003, **73**, 419-428.

11 P.-G. Jönsson and Å. Kvick, *Acta Crystallogr. B*, 1972, **28**, 1827–1833.

12 J. H. Jensen and M. S. Gordon, *J. Am. Chem. Soc.*, 1995, **117**, 8159–8170.

13 R. Ramaekers, J. Pajak, B. Lambie and G. Maes, *J. Chem. Phys.*, 2004, **120**, 4182-4193.

14 Y.-C. Tse, M. D. Newton, S. Visheshwara and J. A. Pople, *J. Am. Chem. Soc.* 1978, **100**, 4329-4331.

15 Y. Ding and K. Krogh-Jespersen, *Chem. Phys. Lett.*, 1992, **199**, 261-266.

16 D. Yu, D. A. Armstrong and A. Rauk, *Can. J. Chem.*, 1992, **70**, 1762-1772.

17 Y. Grenie, J.-C. Lassegues and C. Garrigou-Lagrange, *J. Chem. Phys.*, 1970, **53**, 2980-2982.

18 R. D. Brown, P. D. Godfrey, J. W. V. Storey and M. P. Bassez, *J. Chem. Soc. Chem. Commun.*, 1978, 547-548.

19 Y. Grenie and C.-J. Garrigou-Lagrange, *J. Mol. Spectrosc.*, 1972, **41**, 240-248.

20 R. D. Suenram and F. J. Lovas, *J. Mol. Spectrosc.*, 1978, **72**, 372-382.

21 R. D. Suenram and F. J. Lovas, *J. Am. Chem. Soc.*, 1980, **102**, 7180-7184.

22 F. J. Lovas, Y. Kawashima, J.-U. Grabow, R. D. Suenram, G. T. Freser and E. Hirota, *Astrophys. J.*, 1995, **455**, L201-L204.

23 P. D. Godfrey and R. D. Brown, *J. Am. Chem. Soc.*, 1995, **117**, 2019-2023.

24 I. D. Reva, A. M. Plokhotnichenko, S. G. Stepanian, A. Yu. Ivanov, E. D. Radchenko, G. G. Sheina and Y. P. Blagoi, *Chem. Phys. Lett.*, 1995, **232**, 141-148 (1995); Erratum: *ibid.*, 1995, **235**, 617-617.

25 A. Ivanov, G. Sheina and Y. P. Blagoi, *Spectrochim. Acta A*, 1998, **55**, 219-228.

26 S. G. Stepanian, I. D. Reva, E. D. Radchenko, M. T. S. Rosado, M. L. T. S. Duarte, R. Fausto and L. Adamowicz, *J. Phys. Chem. A*, 1998, **102**, 1041-1054.

27 S. J. McGlone, P. S. Elmes, R. D. Brown and P. D. Godfrey, *J. Mol. Struct.*, 1999, **485-486**, 225-238.

28 R. M. Balabin, *J. Phys. Chem. Lett.*, 2010, **1**, 20-23.

29 C. Espinoza, J. Szczepanski, M. Vala and N. C. Polfer, *J. Phys. Chem. A*, 2010, **114**, 5919-5927.

30 R. M. Balabin, *Phys. Chem. Chem. Phys.*, 2012, **14**, 99-103.

31 G. Bazsó, G. Magyarfalvi and G. Tarczay, *J. Mol. Struct.*, 2012, **1025**, 33-42.

32 G. Bazsó, G. Magyarfalvi and G. Tarczay, *J. Phys. Chem. A*, 2012, **116**, 10539-10547.

33 S. Vishveshwara and J. A. Pople, *J. Am. Chem. Soc.*, 1977, **99**, 2422-2426.

34 H. L. Sellers and L. Schäfer, *J. Am. Chem. Soc.*, 1978, **100**, 7728-7729.

35 P. Palla, C. Petrongolo and J. Tomasi, *J. Phys. Chem.*, 1980, **84**, 435-442.

36 L. Schäfer, H. L. Sellers, F. J. Levas and R. D. Suenram, *J. Am. Chem. Soc.*, 1980, **102**, 6566-6568.

37 L. R. Wright and R. F. Borkman, *J. Am. Chem. Soc.*, 1980, **102**, 6207-6210.

38 C. E. Dykstra, R. A. Chiles and M. D. Garrett, *J. Comput. Chem.*, 1981, **2**, 266-272.

39 S. Millefiori and A. Millefiori, *J. Mol. Struct.*, 1983, **91**, 391-393.

40 K. Siam, V. J. Klimkowski, J. D. Ewbank, C. van Alsenoy and L. Schäfer, *J. Mol. Struct. (TheoChem)*, 1984, **110**, 171-182.

41 M. Ramek, *Int. J. Quantum Chem. Quantum Biol. Symp.*, 1990, **17**, 45-53.

42 M. Ramek, V. K. W. Cheng, R. F. Frey, S. Q. Newton and L. Schäfer, *J. Mol. Struct. (TheoChem)*, 1991, **235**, 1-10.

43 J. H. Jensen and M. S. Gordon, *J. Am. Chem. Soc.* 1991, **113**, 7917–7924.

44 A. G. Császár, *J. Am. Chem. Soc.*, 1992, **114**, 9568-9575.

45 R. F. Frey, J. Coffin, S. Q. Newton, M. Ramek, V. K. W. Cheng, F. A. Momany and L. Schäfer, *J. Am. Chem. Soc.*, 1992, **114**, 5369-5377.

46 C.-H. Hu, M. Shen and H. F. Schaefer, III, *J. Am. Chem. Soc.*, 1993, **115**, 2923-2929.

47 F. Lelj, C. Adamo and V. Barone, *Chem. Phys. Lett.*, 1994, **230**, 189-195.

48 A. G. Császár, *J. Mol. Struct.*, 1995, **346**, 141-152.

49 V. Barone, C. Adamo and F. Lelj, *J. Chem. Phys.*, 1995, **102**, 364-368.

50 D. Yu, A. Rauk and D. A. Armstrong, *J. Am. Chem. Soc.*, 1995, **117**, 1789-1796.

51 S. Hoyau and G. Ohanessian, *J. Am. Chem. Soc.*, 1997, **119**, 2016-2024.

52 D. T. Nguyen, A. C. Scheiner, J. W. Andzelm, S. Sirois, D. R. Salahub and A. T. Hagler, *J. Computat. Chem.*, 1997, **18**, 1609-1631.

53 M. Kieninger, S. Suhai and O. N. Ventura, *J. Mol. Struct. (TheoChem)*, 1998, **433**, 193-201.

54 O. Bludský, J. Chocholoušová, J. Vacek, F. Huisken and P. Hobza, *J. Chem. Phys.*, 2000, **113**, 4629-4635.

55 L. F. Pacios, O. Gálvez and P. C. Gómez, *J. Phys. Chem. A*, 2001, **105**, 5232-5241.

56 T. F. Miller, III and D. C. Clary, *Phys. Chem. Chem. Phys.*, 2004, **6**, 2563-2571.

57 H.-W. Ke, L. Rao, X. Xu and Y.-J. Yan, *J. Theor. Comput. Chem.*, 2008, **7**, 889-909.

58 R. M. Balabin, *Chem. Phys. Lett.*, 2009, **479**, 195-200.

59 H. Kayi, R. I. Kaiser and J. D. Head, *Phys. Chem. Chem. Phys.*, 2011, **13**, 15774-15784.

60 R. A. Cormanich, L. C. Ducati, C. F. Tormena and R. Rittner, Chem. Phys., 2013, **421**, 32-38.

61 V. Barone, M. Biczysko, J. Bloino and C. Puzzarini, *J. Chem. Theory Computat.*, 2013, **9**, 1533-1547.

62 V. Barone, M. Biczysko, J. Bloino and C. Puzzarini, *Phys. Chem. Chem. Phys.*, 2013, **15**, 1358-1363.

63 V. Barone, M. Biczysko, J. Bloino and C. Puzzarini, *Phys. Chem. Chem. Phys.*, 2013, **15**, 10094-10111.

64 B. El Merbouh, M. Bourjila, R. Tijar, R. D. El Bouzaidi, A. El Gridani and M. El Mouhtadi, *J. Theor. Computat. Chem.*, 2014, **13**, 1450067/1-16.

65 M. K. Kesharwani, A. Karton and J. M. L. Martin, *J. Chem. Theory Computat.* 2016, **12**, 444-454.

66 V. Stejfa, M. Fulem and K. Ruzicka, *J. Chem. Phys.*, 2019, **151**, 144504/1-23.

67 E. M. Orjan, A. B. Nacsa and G. Czako, *J. Comput. Chem.*, 2020, **41**, 2001-2014.

68 A. B. Nacsa, G. Czakó, *Phys. Chem. Chem. Phys.*, 2021, **23**, 9663-9671.

69 R. Conte, P. L. Houston, C. Qu, J. Li and J. M. Bowman, *J. Chem.*

Phys., 2020, **153**, 244301/1-11 (2020)

70 Prior studies have used a variety of mutually inconsistent notations for the possible conformers. In the present study, we use a notation that follows the spirit of Cahn-Ingold-Prelog rules (ref. 71): the order of precedence of the three torsions is determined by the molecular weight of the substituents (starting with the terminal atoms of the torsional bond, and adding next levels of neighbours as tie breakers). Hence the three conformational denominators describe, in order, the C-O torsion, the C-N torsion, and the C-C torsion. For the C-O torsion the label approximately describes the relative conformation of the OH group against the C=O group (which has precedence over the C-C bond). The C-N torsion label straightforwardly describes the approximate relative conformation of the CH_2 group against the NH_2 group. For the C-C torsion the label approximately describes the relative conformation of the C-N bond against the C-O(H) bond (the latter having precedence over the C=O bond).

71 R. S. Cahn, *J. Chem. Educ.*, 1964, **41**, 116-125; R. S. Cahn, C. K. Ingold and V. Prelog, *Angew. Chem. Int. Ed.*, 1966, **5**, 385–415; V. Prelog and G. Helmchen, *Angew. Chem. Int. Ed.*, 1982, **21**, 567–583.

72 J. B. Pedley, R. D. Naylor and S. P. Kirby, "Thermochemical Data of Organic Compounds", 2nd ed., Chapman and Hall: London 1986

73 J. D. Cox and G. Pilcher, "Thermochemistry of Organic and Organometallic Compounds", Academic: London 1970

74 H. M. Huffman, S. W. Fox and E. L. Ellis, *J. Am. Chem. Soc.*, 1937, **59**, 2144-2121.

75 H. J. Svec and D. D. Clyde, *J. Chem. Eng. Data*, 1965, **10**, 151-152; D. D. Clyde and H. Svec, “Vapor Pressures of Some Amino Acids”, U. S. Atomic Energy Comm. Report IS-790, Ames Laboratory: Ames 1964.

76 M. Frenkel, G. J. Kabo, K. N. Marsh, G. N. Roganov, and R. C. Wilhoit, "Thermodynamics of Organic Compounds in the Gas State", Vols. 1 and 2, Thermodynamics Research Center: College Station, TX 1994

77 M. L. Frenkel, X. Yan, Q. Dong, and X. Hong, "NIST/TRC Table Database (WinTable 2003)", NIST Std. Ref. Database 85, National Institute of Standards and Technology: Gaithersburg, MD 2003

78 D. D. Wagman, W. H. Evans, V. B. Parker, R. H. Schumm, I. Halow, S. M. Bailey, K. L. Churney and R. L. Nuttall, "The NBS Tables of Chemical Thermodynamic Properties", *J. Phys. Chem. Ref. Data*, 1982, **11**, Suppl. 2 (1982)

79 The NBS Tables (ref. 78) and the NBS Technical Note 270 (ref. 80) do not provide explicitly the uncertainties, but stipulate that the implied accuracy is given by the number of digits shown. The NBS Technical Note 270, which use cal as units, indicates that the expected uncertainty is in the range of 1 to 10 of the least significant digit shown; the transition to J as units in the NBS Tables led to declaring the expected uncertainties to be in the range of 4 to 40 of the last digit.

80 D. D. Wagman, W. H. Evans, I. Halow, V. B. Parker, S. M. Bailey, and R. H. Schumm, "Selected Values of Chemical Thermodynamic Properties. Tables for the First Thirty-Four Elements in the Standard Order of Arrangement", NBS Technical Note 270-3, U.S. Gov. Printing Office: Washington, DC 1968

81 E. L. Dias, E. S. Domalski and J. C. Colbert, *J. Chem. Thermodyn.*, 1992, **24**, 1311–1318.

82 P. J. Linstrom and W. G. Mallard, Eds., “NIST Chemistry WebBook”, NIST SRD 69, National Institute of Standards and Technology: Gaithersburg 2023, accessed April 2024

83 S. N. Ngauv, R. Sabbah and M. Laffitte, *Thermochim. Acta*, 1977, **20**, 371-380.

84 V. P. Vasil’ev, V. A. Borodin and S. B. Kopnyshev, *Russ. J. Phys. Chem.*, 1991, **65**, 29-32.

85 J. O. Hutchens, A. G. Cole and J. W. Stout, *J. Phys. Chem.*, 1963, **67**, 1128-1130.

86 T. Tsuzuki, D. O. Harper and H. Hunt, *J. Phys. Chem.*, 1958, **62**, 1594-1595.

87 A. G. Emery and F. G. Benedict, *Am. J. Physiol.*, 1911, **28**, 301-307.

88 F. Wrede, *Z. phys. Chem.*, 1911, **75**, 81-94.

89 E. Fischer and F. Wrede, *Sitzungsber. Dtsch. Akad. Wiss. Berlin Kl. Math. Phys. Tech.*, 1904, 687-715.

90 P. Lemoult, *Compt. rend.*, 1904, **139**, 633-635.

91 M. Berthelot and G. Andre, *Ann. Chim. Phys.*, 1891, **22**, 5-52.

92 F. Stohmann, *J. Prakt. Chem.*, 1885, **31**, 273-306.

93 F. Stohmann and H. Langbein, *J. Prakt. Chem.*, 1891, **44**, 336-399.

94 B. Ruscic and D. H. Bross, *Computer Aided Chem. Eng.*, 2019, **45**, 3-114.

95 B. Ruscic, *Int. J. Quantum Chem.*, 2014, **114**, 1097-1101.

96 By a universally accepted convention in thermochemistry, the listed uncertainties correspond to 95% confidence intervals (see refs. 94 and 95). This enables the notion that if two values for the same thermochemical quantity differ by more than their combined uncertainties, it is highly probable that at least one value is incorrect.

97 D. Feller, D. H. Bross and B. Ruscic, *J. Phys. Chem. A*, 2017, **121**, 6187–6198.

98 D. Feller, D. H. Bross and B. Ruscic, *J. Phys. Chem. A*, 2019, **123**, 3481–3496.

99 The vaporization (or sublimation) enthalpies need to be corrected for real-ideal gas differences by accounting for the contributions of dimers, trimers, etc. in the gas phase [see refs. 94, 100 and 101]. However, this correction is negligible if the equilibrium vapor pressure is sufficiently low, as is in the case of glycine.

100 B. Ruscic, *J. Phys. Chem. A*, 2013, **117**, 11940–11953.

101 V. Majer, V. Svoboda and H. V. Kehiaian, "Enthalpies of Vaporization of Organic Compounds: A Critical Review and Data Compilation", IUPAC Chem. Data Ser. No. 32, Blackwell: Oxford 1985

102 S. Takagi, H. Chihara and S. Seki, *Bull. Chem. Soc. Jpn.*, 1959, **32**, 84-88.

103 C. G. de Kruif, J. Voogd and J. C. A. Offringa, *J. Chem. Thermodyn.*, 1979, **11**, 651-656.

104 It is possible that the value 153.2 ± 4.2 kJ mol^{-1} listed by Pedley et al. (ref. 72) is a typo and 135.2 ± 4.2 kJ mol^{-1} was actually intended (although the converted value in kcal mol^{-1} given by Pedley et al., 36.61 ± 1.00, matches the former).

105 B. Ruscic and D. H. Bross, *Mol. Phys.*, 2021, **119**, e1969046/1-17.

106 D. H. Bross, H. G. Yu, L. B. Harding and B. Ruscic, *J. Phys. Chem. A*, 2019, **123**,4212-4231.

107 A. Tajti, P. G. Szalay, A. G. Császár, M. Kállay, J. Gauss, E. F. Valeev, B. A. Flowers, J. Vázquez and J. F. Stanton, *J. Chem. Phys.*, 2004, **121**, 11599-11613.

108 Y. J. Bomble, J. Vázquez, M. Kállay, C. Michauk, P. G. Szalay, A. G. Császár, J. Gauss and J.F. Stanton, *J. Chem. Phys.*, 2006, **125**, 064108/1-8

109 M. E. Harding, J. Vázquez, B. Ruscic, A. K. Wilson, J. Gauss

and J. F. Stanton, *J. Chem. Phys.*, 2008, **128**, 114111/1-15.

110 J. H. Thorpe, C. A. Lopez, T. Lam Nguyen, J. H. Baraban, D. H. Bross, B. Ruscic and J. F. Stanton, *J. Chem. Phys.* 2019, **150**, 224102/1-16.

111 J. H. Thorpe, J. L. Kilburn, D. Feller, P. B. Changala, D. H. Bross, B. Ruscic and J. F. Stanton, *J. Chem. Phys.*, 2021, **155**, 184109/1-13.

112 A. Karton, E. Rabinovich, J. M. L. Martin and B. Ruscic, *J. Chem. Phys.*, 2006, **125**, 144108/1-17.

113 A. Karton, P. R. Taylor and J. M. L. Martin, *J. Chem. Phys.*, 2007, **127**, 064104/1-11.

114 E. Semidalas, A. Karton and J. M. L. Martin, *J. Phys. Chem. A*, 2024, **128**, 1715-1724.

115 A. G. Császár, W. D. Allen and H. F. Schaefer, III, *J. Chem. Phys.*, 1998, **108**, 9751-9764.

116 A. L. L. East and W. D. Allen, *J. Chem. Phys.*, 1993, **99**, 4638-4650.

117 J. P. Kenny, W. D. Allen and H. F. Schaefer, III, *J. Chem. Phys.*, 2003, **118**, 7353-7365.

118 M. S. Schuurman, S. R. Muir, W. D. Allen and H. F. Schaefer, III, *J. Chem. Phys.*, 2004, **120**, 11586-11599.

119 S. E. Wheeler, K. A. Robertson, W. D. Allen, H. F. Schaefer, III, Y. J. Bomble and J.F. Stanton, *J. Phys. Chem. A*, 2007, **111**, 3819-3830.

120 S. E. Wheeler, W. D. Allen and H. F. Schaefer, III, *J. Chem. Phys.*, 2004, **121**, 8800-8813.

121 B. Ruscic, D. Feller, D. A. Dixon, K. A. Peterson, L. B. Harding, R. L. Asher and A. F. Wagner, *J. Phys. Chem. A*, 2001, **105**, 1-4.

122 B. Ruscic, A. F. Wagner, L. B. Harding, R. L. Asher, D. Feller, D. A. Dixon, K. A. Peterson, Y. Song, X. Qian, C.-Y. Ng, J. Liu, W. Chen and D. W. Schwenke, *J. Phys. Chem. A*, 2002, **106**, 2727-2747.

123 D. Feller, K. A. Peterson and D.A. Dixon, *J. Chem. Phys.*, 2008, **129**, 204105/1-32.

124 D. A. Dixon, D. Feller and K. A. Peterson, *Annu. Rev. Comput. Chem.*, 2012, **8**, 1-28.

125 D. Feller, K. A. Peterson and D. A. Dixon, *Mol. Phys.*, 2012, **110**, 2381-2399.

126 K. A. Peterson, D. Feller and D. A. Dixon, *Theor. Chem. Acc.*, 2012, **131**, 1079/1-20.

127 D. Feller, K. A. Peterson and B. Ruscic, *Theor. Chem. Acc.*, 2014, **133**, 1407/1-16.

128 S. J. Klippenstein, L. B. Harding and B. Ruscic, *J. Phys. Chem. A*, 2017, **121**, 6580-6602.

129 J. A. Montgomery, Jr., M. J. Frisch, J. W. Ochterski and G. A. Petersson, *J. Chem. Phys.*, 1999, **110**, 2822-2827.

130 J. A. Montgomery, Jr., M. J. Frisch, J. W. Ochterski, and G. A. Petersson, *J. Chem. Phys.*, 2000, **112**, 6532-6542.

131 J. W. Ochterski, G. A. Petersson and J. A. Montgomery, Jr., *J. Chem. Phys.*, 1996, **104**, 2598-2619.

132 L. A. Curtiss, P. C. Redfern, K. Raghavachari and J. A. Pople, *J. Chem. Phys.*, 2001, **114**, 108–117.

133 L. A. Curtiss, P. C. Redfern and K. Raghavachari, *J. Chem. Phys.*, 2007, **126**, 084108/1-12.

134 J. M. L. Martin and G. de Oliveira, *J. Chem. Phys.*, 1999, **111**, 1843-1856.

135 S. Parthiban and J. M. L. Martin, *J. Chem. Phys.*, 2001, **114**, 6014-6029.

136 Standard mid-level composite approaches, such as, for example, CBS-QB3, CBS-APNO, G3X, G4, and even W1, are not capable of achieving even chemical accuracy (± 1 kcal mol^{-1} or ± 4 kJ mol^{-1}), at least when used to produce an enthalpy of formation by directly converting the computed total atomization energy, in spite of reoccurring claims in the literature to the contrary. As discussed in ref. 95, such claims are typically based on the benchmarked mean absolute deviations (MAD) for these methods, which severely underestimate the universally followed level of expression of uncertainty in thermochemistry (which should correspond to 95% confidence intervals).

137 The illustrative values for $\Delta_fH°_{298}$(glycine $_{(g)}$) listed here were obtained by adding the difference [$\Delta_fH°_{298}$(glycine $_{(g)}$) - $\Delta_fH°_0$(glycine $_{(g)}$)] = -17.023 kJ mol^{-1} (obtained from the current partition functions) to $\Delta_fH°_0$(glycine $_{(g)}$) that was obtained directly from the computed 0 K total atomization energy.

138 O. V. Dorofeeva and O. N. Ryzhova, *J. Chem. Thermodyn.*, 2009, **41**, 433-437.

139 O. V. Dorofeeva and O. N. Ryzhova, *J. Phys. Chem. A*, 2014, **118**, 3490–3502.

140 G. Bouchoux, S. Huang, and B. S. Inda, *Phys. Chem. Chem. Phys.* 2011, **13**, 651–668.

141 M. L. Stover, V. Jackson, M. Matus, M. Adams, C. J. Cassady, and D. A. Dixon, *J. Phys. Chem. B*, 2012, **116**, 2905–2916.

142 A. Karton, L.-J. Yu, M. K. Kesharwani and J. M. L. Martin, *Theor. Chem. Acc.* 2014, **133**, 1483/1-15.

143 A. D. Becke, *J. Chem. Phys.*, 1993, **98**, 5648-5652; C. Lee, W. Yang and R. G. Parr, *Phys. Rev. B*, 1988, **37**, 785-789; S. H. Vosko, L. Wilk and M. Nusair, *Can. J. Phys.*, 1980, **58**, 1200-1211; P. J. Stephens, F. J. Devlin, C. F. Chabalowski and M. J. Frisch, *J. Phys. Chem.*, 1994, **98**, 11623-11627.

144 K. Raghavachari, J. S. Binkley, R. Seeger and J. A. Pople, *J. Chem. Phys.*, 1980, **72**, 650-654.

145 A. Karton and J. M. L. Martin, *J. Chem. Phys.*, 2012, **136**, 124114/1-12.

146 B. Ruscic, R. E. Pinzon, M. L. Morton, G. von Laszewski, S. J. Bittner, S. G. Nijsure, K. A. Amin, M. Minkoff and A. F. Wagner, *J. Phys. Chem. A*, 2004, **108**, 9979–9997.

147 B. Ruscic, R. E. Pinzon, G. von Laszewski, D. Kodeboyina, A. Burcat, D. Leahy, D. Montoya and A. F. Wagner, *J. Phys. Conf. Ser.*, 2005, **16**, 561–570

148 B. Ruscic, "Active Thermochemical Tables", in: 2005 Yearbook of McGraw-Hill Encyclopaedia of Science and Technology, McGraw-Hill: New York 2004.

149 B. Ruscic, R. E. Pinzon, M. L. Morton, N. K. Srinivasan, M.-C. Su, J. W. Sutherland, and J. V. Michael, *J. Phys. Chem. A* 2006, **110**, 6592-6601.

150 Rather than being absolute, the constraints are qualified by their accompanying uncertainties.

151 PuRe Data Resources at a Glance, https://science.osti.gov/Initiatives/PuRe-Data/Resources-at-a-Glance, accessed April 2024

152 "Active Thermochemical Tables (ATcT) Advance Chemistry as a PuRe Data Resource", U.S. Department of Energy Office of Science, press release on March 20, 2023; https://www.energy.gov/science/articles/active-thermochemical-tables-atct-advance-chemistry-pure-data-resource

153 "Department of Energy Recognizes Two Decades' Worth of Argonne's High-Quality Thermochemical Data", Argonne National Laboratory, Lemont, Illinois, press release on March 20, 2023; https://www.anl.gov/article/department-of-energy-recognizes-two-decades-worth-of-argonnes-highquality-thermochemical-data

154 The cited pageview statistic is based on an analysis of the

calendar year 2023 webserver logs of the https://ATcT.anl.gov website.

155 B. Ruscic and D. H. Bross, “Active Thermochemical Tables (ATcT) values based on ver. 1.130 of the Thermochemical Network”, Argonne National Laboratory, Lemont, Illinois 2023; available at ATcT.anl.gov; DOI: 10.17038/CSE/1997229

156 N. Genossar, P. B. Changala, B. Gans, J.-C. Loison, S. Hartweg, M.-A. Martin-Drumel, G. A. Garcia, J. F. Stanton, B. Ruscic and J. H. Baraban, *J. Am. Chem. Soc.*, 2022, **144**, 18518-18525.

157 J. H. Thorpe, D. Feller, D. H. Bross, B. Ruscic and J. F. Stanton, *Phys. Chem. Chem. Phys.*, 2023, **25**, 21162–21172.

158 T. L. Nguyen, J. Peeters, J.-F. Müller, A. Perera, D. H. Bross, B. Ruscic and J. F. Stanton, Proc. Natl. Acad. Sci., 2023, **120**, e2304650120/1-8.

159 N. A. Seifert, B. Ruscic, R. Sivaramakrishnan and K. Prozument, *J. Mol. Spectrosc.*, 2023, **398**, 111847/1-8

160 U. Jacovella, B. Ruscic, N. L. Chen, H.-L. Le, S. Boyé-Péronne, S. Hartweg, M. Roy-Chowdhury, G. A. Garcia, J.-C. Loison and B. Gans, *Phys. Chem. Chem. Phys.*, 2023, **25**, 30838-30847.

161 B. Ruscic and D. H. Bross, “Active Thermochemical Tables (ATcT) values based on ver. 1.202 of the Thermochemical Network”, Argonne National Laboratory, Lemont, Illinois 2024

162 L. V. Gurvich, I. V. Veyts and C. B. Alcock, "Thermodynamic Properties of Individual Substances", 4th ed., Vol. 1, Parts 1 and 2, Hemisphere: New York 1989.

163 F. Huisken, O. Werhahn, A. Y. Ivanov and S. A. Krasnokutski, *J. Chem. Phys.*, 1999, **111**, 2978-2984.

164 V. Barone, *J. Chem. Phys.*, 2005, **122**, 014108/1-10.

165 J. Bloino, M. Biczysko and V. Barone, *J. Chem. Theory Comput.*, 2012, **8**, 1015-1036.

166 D. T. Colbert and W. H. Miller, *J. Chem. Phys.*, 1992, **96**, 1982-1991.

167 M. J. Frisch, G. W. Trucks, H. B. Schlegel, G. E. Scuseria, M. A. Robb, J. R. Cheeseman, G. Scalmani, V. Barone, G. A. Petersson, H. Nakatsuji, X. Li, M. Caricato, A. V. Marenich, J. Bloino, B. G. Janesko, R. Gomperts, B. Mennucci, H. P. Hratchian, J. V. Ortiz, A. F. Izmaylov, J. L. Sonnenberg, D. Williams-Young, F. Ding, F. Lipparini, F. Egidi, J. Goings, B. Peng, A. Petrone, T. Henderson, D. Ranasinghe, V. G. Zakrzewski, J. Gao, N. Rega, G. Zheng, W. Liang, M. Hada, M. Ehara, K. Toyota, R. Fukuda, J. Hasegawa, M. Ishida, T. Nakajima, Y. Honda, O. Kitao, H. Nakai, T. Vreven, K. Throssell, J. A. Montgomery, Jr., J. E. Peralta, F. Ogliaro, M. J. Bearpark, J. J. Heyd, E. N. Brothers, K. N. Kudin, V. N. Staroverov, T. A. Keith, R. Kobayashi, J. Normand, K. Raghavachari, A. P. Rendell, J. C. Burant, S. S. Iyengar, J. Tomasi, M. Cossi, J. M. Millam, M. Klene, C. Adamo, R. Cammi, J. W. Ochterski, R. L. Martin, K. Morokuma, O. Farkas, J. B. Foresman and D. J. Fox, “Gaussian 09”, Gaussian, Inc., Wallingford CT: 2016

168 R. A. Kendall, T. H. Dunning, Jr. and R. J. Harrison, *J. Chem. Phys.*, 1992, **96**, 6796-6806.

169 D. Rowland, *J. Phys. Chem. Ref. Data*, 2018, **47**, 023104/1-15.

170 G. S. Parks, H. M. Huffman and M. Barmore, *J. Am. Chem. Soc.*, 1933, **55**, 2733-2740.

171 J. O. Hutchens, A. G. Cole and J. W. Stout, *J. Am. Chem. Soc.*, 1960, **82**, 4813-4815.

172 V. A. Drebushchak, Yu. A. Kovalevskaya, I. E. Paukov and E. V. Boldyreva, *J. Thermal Anal. Calorim.*, 2003, **74**, 109–120.

173 D. G. Archer, *J. Phys. Chem. Ref. Data*, 1992, **21**, 1-21; D. G. Archer, *J. Phys. Chem. Ref. Data*, 1999, **28**, 1-17; D. G. Archer, *J. Phys. Chem. Ref. Data*, 2000, **29**, 1141-1156.

174 V. A. Drebushchak, E. V. Boldyreva, Yu. A. Kovalevskaya, I. E. Paukov and T. N. Drebushchak, *J. Thermal Anal. Calorim.*, 2005, **79**, 65-70.

175 B. Ruscic, J. E. Boggs, A. Burcat, A. G. Császár, J. Demaison, R. Janoschek, J. M. L. Martin, M. L. Morton, M. J. Rossi, J. F. Stanton, P. G. Szalay, P. R. Westmoreland, F. Zabel and T. Bérces, *J. Phys. Chem. Ref. Data*, 2005, **34**, 573–656.

176 Of course, for each torsional level, the sum of fractional weights over all conformers visited by the torsional motion equals one, since each torsional function is normalized.

177 A. Karton, B. Ruscic, and J. M. L. Martin, J. Mol. Struct. (TheoChem), 2007, **811**, 345-353.

178 V. Kasalová, W. D. Allen, H. F. Schaefer III, E. Czinki and A. G. Császár, *J. Comput. Chem.*, 2007, **28**, 1373-1383.

179 Curiously, after correction to constant pressure, the $\Delta_{combust}H°_{298}(\alpha$-glycine) of Tsuzuki et al. (ref. 86) seems to imply $\Delta_f H°_{298}(\alpha$-glycine) = -536.1 ± 1.0 kJ mol^{-1} (rather than -537.2 kJ mol^{-1} reported by Hutchens et al., ref. 85).

180 B. Ruscic, D. Feller and K. A. Peterson, *Theor. Chem. Acc.*, 2014, **133**, 1415/1-12.

181 Note that because of the bias introduced by the thermochemical convention that is artificially fixing the enthalpy of formation and the free energy of formation of $H^+_{(aq)}$ to zero, as if it were a new reference element, the difference between the enthalpy of formation of a gas phase ion and its conventional aqueous enthalpy of formation does not correspond to its solvation enthalpy (see discussion in ref. 94).

182 The free energy of dissolution of α-glycine to undissociated aqueous glycine is related to the corresponding Henry’s law constant, $k°_H$. Similarly, the corresponding enthalpy of dissolution is related to the first derivative of the natural logarithm of Henry’s law constant against the inverse temperature, $d(\ln(k°_H))/d(1/T)$.

183 G. C. Kresheck, H. Schneide, and H. A. Scheraga, *J. Phys. Chem.*, 1965, **69**, 3132-3144.

184 C. H. Spink and I. Wadso, *J. Chem. Thermodyn.*, 1975, **7**, 561-572.

185 M. Abu-Hamdiyyah and A. Shehabuddin, *J. Chem. Eng. Data*, 1982, **27**, 74-76.

186 B. Palecz and S. Taniewska-Osinska, *Thermochim. Acta*, 1990, **173**, 295-299.

187 S. L. Miller and D. Smith-Magowan, *J. Phys. Chem. Ref. Data*, 1990, **19**, 1049-1073.

188 B. Palecz, *J. Therm. Anal.*, 1998, **54**, 257-263.

189 V. G. Badelin, V. I. Smirnov and I. Mezhevoy, *Zh. Fiz. Khim.*, 2002, **76**, 1299-1302.

190 V. P. Korolev, D. V. Batov, N. L. Smirnova and A. V. Kustov, *Russ. Chem. Bull.*, 2007, **56**, 739-742; V. P. Korolev, D. V. Batov, N. L. Smirnova and A. V. Kustov, *J. Struct. Chem.*, 2007, **48**, 666-672.

191 X. Qiu, Q. Lei, W. Fang and R. Lin, *J. Chem. Eng. Data*, 2009, **54**, 1426-1429.

192 E. V. Grigorova, L. P. Bondareva, A. V. Kadantsev, Y. A. Byvaltsev, V. V. Khripushin and T. S. Kornienko, *Russ. J. Phys. Chem. A*, 2010, **84**, 1636-1639.

193 B. B. Owen, *J. Am. Chem. Soc.*, 1934, **56**, 24-27.

194 E. J. King, *J. Am. Chem. Soc.*, 1951, **73**, 155-159.

195 S. P. Datta and A. K. Grzybowski, *Trans. Faraday Soc.*, 1958, 54, 1179-1187; *ibid.*, 1958, **54**, 1188-1194.

196 M. A. Marini, R. L. Berger, D. P. Lam and C. J. Martin, *Anal. Biochem.*, 1971, **43**, 188-198.

This journal is © The Royal Society of Chemistry 20xx

197 E. S. Hamborg, J. P. M. Niederer and G. F. Versteeg, *J. Chem. Eng. Data*, 2007, **52**, 2491-2502.
198 B. P. Dey and S. C. Lahiri, *J. Ind. Chem. Soc.*, 2010, **87**, 29-41.
199 The free energy of dissociation of undissociated aqueous glycine (aq, undiss.) to fully dissociated glycine (aq), the latter being identical to $NH_2CH_2C(O)O^-$ (aq) + H^+ (aq), is related to the second dissociation constant of aqueous glycine (aq, undiss.). The first dissociation constant of aqueous glycine usually refers to the dissociation of protonated aqueous glycine, $NH_3CH_2C(O)OH^+$ (aq) to undissociated aqueous glycine (aq, undiss.).
200 A. Karton, S. Daon and J. M. L. Martin, *Chem. Phys. Lett.*, 2011, **510**, 165-178.
201 Curation implies, *inter alia*, critical evaluation and - when necessary – reinterpretation both of the originally determined value and its likely uncertainty.

The current version of ATcT results, together with detailed analyses of provenance and cross-correlation for each species, will become shortly available on the ATcT website, ATcT.anl.gov

All other raw data are archived at Argonne National Laboratory and is available for inspection upon reasonable request.